forests

MDPI

Article

Modeling Migratory Flight in the Spruce Budworm: Temperature Constraints

Jacques Régnière [1,*], Johanne Delisle [1], Brian R. Sturtevant [2], Matthew Garcia [3] and Rémi Saint-Amant [1]

1 Natural Resources Canada, Canadian Forest Service, Québec, QC G1V 4C7, Canada; johanne.delisle@canada.ca (J.D.); remi.st-amant@canada.ca (R.S.-A.)
2 USDA-Forest Service, Northern Research Station, Rhinelander, WI 54501, USA; brian.r.sturtevant@usda.gov
3 Department of Forest and Wildlife Ecology, University of Wisconsin-Madison, Madison, WI 53706, USA; Matt.E.Garcia@gmail.com
* Correspondence: Jacques.Regniere@Canada.ca; Tel.: +1-418-648-5257

Received: 30 July 2019; Accepted: 9 September 2019; Published: 13 September 2019

Abstract: We describe an individual-based model of spruce budworm moth migration founded on the premise that flight liftoff, altitude, and duration are constrained by the relationships between wing size, body weight, wingbeat frequency, and air temperature. We parameterized this model with observations from moths captured in traps or observed migrating under field conditions. We further documented the effects of prior defoliation on the size and weight (including fecundity) of migrating moths. Our simulations under idealized nocturnal conditions with a stable atmospheric boundary layer suggest that the ability of gravid female moths to migrate is conditional on the progression of egg-laying. The model also predicts that the altitude at which moths migrate varies with the temperature profile in the boundary layer and with time during the evening and night. Model results have implications for the degree to which long-distance dispersal by spruce budworm might influence population dynamics in locations distant from outbreak sources, including how atmospheric phenomena such as wind convergence might influence these processes. To simulate actual migration flights en masse, the proposed model will need to be linked to regional maps of insect populations, a phenology model, and weather model outputs of both large- and small-scale atmospheric conditions.

Keywords: spruce budworm; *Choristoneura fumiferana*; moth; Lepidoptera; forest protection; early intervention strategy; migration; simulation; aerobiology

1. Introduction

Long-distance migration and dispersal behaviors are fundamental life history traits across a broad range of insect taxa [1]. Long-distance movements enable insect species to accommodate seasonal phenology of food resources and to escape local predation pressure, inadequate or devastated resources, and other environmental stressors [2], and thus constitute a fundamental mechanism for "spreading the risk" throughout the population [3]. Migration behavior is typified by temporary suspension of other base functions such as foraging, habitat-searching, and mate-finding to allow sustained and directionally consistent movements [4], generally during the winged (adult) development stage [1]. Virtually any insect species entering flight will be subject to a series of physical and physiological constraints affecting migration success, resulting in diverse physiological and behavioral adaptations. Radar studies across several decades have demonstrated the prevalence of long-distance migration aided by high wind speeds near the top of the atmospheric boundary layer, especially for nocturnal insect flights [5,6]. Understanding the main factors that control insect aerial migration could provide a way to predict migratory movements, which is particularly important in the case of economically

important outbreak species exhibiting long-distance migration and dispersal behavior such as acridid locusts [7] and other agricultural pests such as the fall armyworm (*Spodoptera frugiperda* Smith) [8].

One of the most intensely studied forest insects in terms of its aerobiology is the spruce budworm (SBW), *Choristoneura fumiferana* (Clem.) [9], the larvae of which periodically defoliate spruce (*Picea* spp.) and balsam fir (*Abies balsamea* L.) across broad regions of the North American boreal forest [10]. Endemic populations of the SBW are subject to mate-finding and demographic Allee effects [11,12], and immigrant males may improve the odds of local females finding a mate. Immigrant gravid females can also help the local population overcome the demographic Allee effect [12]. Both processes could facilitate the spatial spread of outbreaks. Understanding the main factors that control long-distance transport of SBW and other species can thus help interpret the spatiotemporal dynamics of insect outbreaks. SBW moths do not feed, and females emerge with their full egg complement. Females mate prior to migration, and both males and females participate in mass migratory behavior [9]. Observations indicate that fully gravid females are generally too heavy to fly, and thus lay part of their eggs locally prior to undertaking long-distance flight [13,14]. Exceptions can occur in conditions of highly depleted food resources, where starved females carrying smaller egg complements may emigrate without first laying eggs [15,16].

SBW falls into a class of flying insects that initiate exodus flight around sunset and dusk (see the work of [17]) and tend to fly within and near the relatively stable nocturnal boundary layer, often associated with a near-surface temperature inversion [18]. Budworm moths are strong fliers, launching into the wind during a rapid-ascent flight phase before transitioning to a common downwind orientation [9]. As in other nocturnal migrants, migrating SBW moths have been observed to stratify within one or more vertical layers in the atmospheric boundary layer [6,18]. Those altitudes often correspond with higher wind speeds that increase displacement velocity and ultimate dispersal distance (e.g., the work of [19]), generally over tens to hundreds of kilometers in a single night [20,21].

In previous research, Sturtevant et al. [21] synthesized knowledge of SBW aerobiology to develop a Lagrangian agent-based model of long-distance aerial dispersal. That model produced realistic moth flight trajectories and deposition patterns that were consistent with ground-based trapping surveys. However, the authors applied several simple empirical functions to accommodate some highly uncertain processes, including static distributions of both cruising altitudes and durations of moth flight. Improvements on that model would relate the ability of moths to a rise in the air profile according to the underlying moth physiology and atmospheric structure that drive such flight behavior, leading to more dynamic vertical distributions of migrating SBW, as observed in nature [9]. The compositions of migrant layers in terms of sex ratio, size, and egg load carried by females in flight then become emergent properties of the individual-based model, rather than prescribed parameters.

In this paper, we describe a combined mathematical and empirical framework for the simulation of insect migratory flight behaviors including liftoff conditions, flight altitude, and landing based on air temperature and adult SBW physical characteristics including wing size and body weight. SBW is highly suitable for this approach because so much is known about its migratory behavior and there is a renewed appreciation of the importance of migration in its population dynamics. This is the first in a series of papers where we build upon a previous modeling framework [21] to develop a more sophisticated process-based solution with which we can simulate moth migration events. The ultimate objective of this work is to develop a simulation model that will allow the prediction, in near-real-time, of the spread of the insect's populations through moth migration and subsequent oviposition. We aim for a model that takes into account source population distribution and density, seasonal phenology including the progression of reproduction, circadian rhythm, and interactions with meteorological conditions at the surface (i.e., in the host forest stands) and within the lowest 1 km of the atmospheric boundary layer.

2. Model Construction

2.1. Modeling Approach

The physics of insect flight is a complex subject [22]. As a simplifying assumption, to avoid a very large number of details for which little data exist, we consider three main factors that determine the ability of a winged moth to generate the forces required to lift off and move by flight: body weight, wing surface area, and wingbeat frequency. We then relate wingbeat frequency to temperature to obtain a temperature-dependent model of flight capacity. In the SBW, several factors affect body size (wing area) and weight, and thus flight. Males are typically smaller and lighter than females. In females, body weight is also determined by reproductive status. Gravid females deposit their eggs gradually in successive masses of diminishing size [23], such that the weight of a female drops considerably during her lifetime [24]. In addition, fecundity (and thus body weight) depends on the quality and quantity of food the female was able to acquire during larval development [25]. Food availability is strongly affected in turn by defoliation intensity, a function of population density, which influences adult size and weight in both sexes [15]. SBW moths also lose weight as they consume stored energy reserves, a topic of current research not included in this model. Our individual-based model thus requires both empirical relationships and associated distributions among these SBW adult moth morphometrics and their underlying drivers.

2.2. Morphometric Relationships

We obtained data (weight, forewing surface area, fecundity) on individual moths either collected as pupae from host foliage or caught daily in canopy traps suspended well above the top of host trees at Lac des Huit-Milles, Quebec, Canada, in the summers of 1989 and 1990. The canopy traps used were described in detail by Eveleigh et al. [24]. We also collected moths in light traps (Model 2851U, BioQuip Products, Rancho Dominguez, CA, USA) at 2- to 4-day intervals in the lower St. Lawrence region of Quebec, Canada, between 2010 and 2015. Throughout this paper, we use dry weight as a measure of insect mass. All weight measurements were obtained after desiccating the insects for 24 h at 70 °C. The values of all weight-related parameters thus implicitly account for the missing water content of moths. This assumes that the relative water content of moth bodies remains constant. We also use the area of a single forewing as an index of total wing area, realizing that actual wing area in moths is composed of two forewings and two hindwings.

2.2.1. Female Fecundity, Weight, Wing Area, and Influence of Defoliation

We collected SBW pupae in the Lac des Huit-Milles stand on host foliage during 1989–1990 to determine the forewing surface area and dry weight of 122 fully gravid and 132 fully spent females (which were allowed to lay eggs until their death in the laboratory). Host defoliation (current-year foliage) averaged 64% in 1989–1990 in the stand. From the fully spent females in this sample, we established a relationship between potential fecundity (E, in eggs per female) and forewing surface area (A, in cm^2) as follows:

$$E = 739.2A^{1.758}\varepsilon \left(R^2 = 0.45\right), \quad (1)$$

(Figure 1a) where ε is a lognormal error term (Anderson-Darling test of normality [26] AD = 0.324; $p = 0.52$). Observed fecundity E_d, where the level of defoliation is known, can be corrected to provide an estimate of potential fecundity in the absence of defoliation, E_0, using the relationship between defoliation d (a proportion between 0 and 1) and fecundity reported in the work of [25]:

$$E_0 = E_d/(1 - 117d/216.8), \quad (2)$$

which is represented for $d = 0.64$ by the dotted line in Figure 1a.

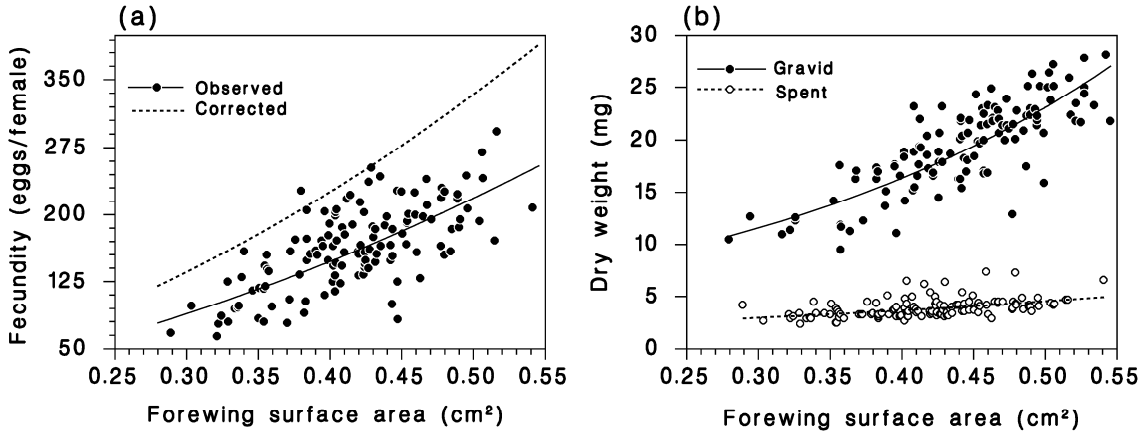

Figure 1. (**a**) Relationship between forewing surface area and lifetime fecundity among females collected as pupae on balsam fir foliage (64% defoliation) at Lac des Huit-Milles, 1989–1990 (solid line: Equation (1); dotted line: after correction for defoliation using Equation (2)). (**b**) Relationship between forewing surface area and dry weight of fully gravid and spent females (lines: Equation (3)), pupae collected at Lac des Huit-Milles, 1989–1990.

The dry weights (M, in g) of gravid and spent females were vastly different because of the weight of eggs (Figure 1b), with fully-gravid females at 0.0194 ± 0.0042 g (standard deviation) and spent females at 0.0039 ± 0.0009 g. A mixed-effects regression accurately described the relationship between dry weight and wing area among the fully gravid and fully spent females:

$$M = e^{-6.4648+0.9736G+2.14A+1.3049GA}\varepsilon \left(R^2 = 0.95\right), \quad (3)$$

using gravidity $G = E/E_0$ as a continuous variable in the range 0 (fully spent, $E = 0$) to 1 (containing its full potential fecundity, $E = E_0$), and with ε near-lognormal with mean = 1 and standard deviation 0.16 ($n = 254$; AD = 1.675; $p < 0.005$). In the model, the weight of females is related to their remaining fecundity (unlaid eggs), and because defoliation decreases initial fecundity (by the ratio E_d/E_0), it reduces their weight correspondingly. The weight of males is also reduced by the same ratio (1–117d/216.8) in areas of known defoliation [15].

Among female SBW moths caught in light traps in the lower St. Lawrence region of Quebec, Canada, between 2010 and 2015, the year of capture explained 37% of the total variability in forewing surface area (analysis of variance (ANOVA) F = 6.74; df = 5, 47; $p < 0.001$). Although statistically significant, the relationship with stand-level defoliation explained only 8.6% of the total variability (F = 7.84; df = 1, 47; $p = 0.007$). There was no significant interaction between year and defoliation (F = 1.53; df = 1, 42; $p = 0.202$). Because the effect of defoliation on forewing area was small, only 0.02 cm^2 over the range of 0% to 100% defoliation (Figure 2), we chose to ignore this factor in the final flight model. Thus, in our model, defoliation has an influence only on the moth weight, and individuals that were submitted to starvation due to overcrowding have larger wings relative to their body weight than well-fed ones, and are thus more apt to emigrate.

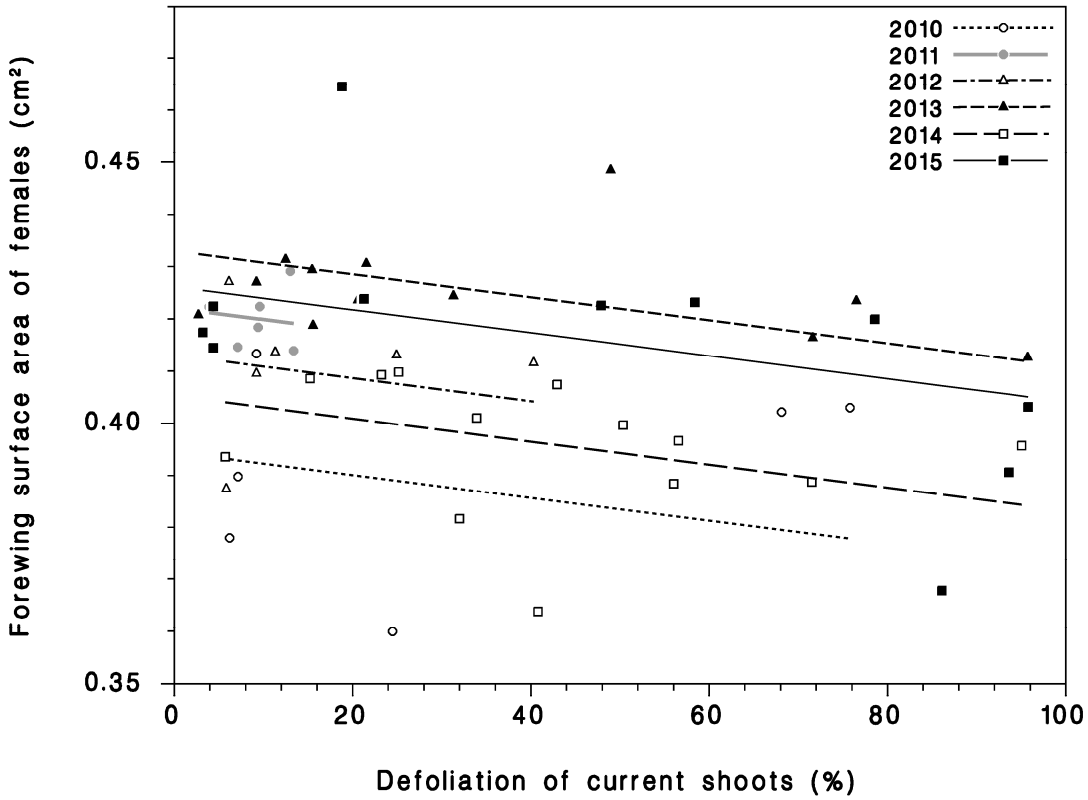

Figure 2. Effect of year and current-shoot defoliation on forewing surface area among female moths caught in light traps in the lower St. Lawrence region, 2010–2015. Lines are linear least-squares regressions fitted to the observations available for each year.

2.2.2. Moths Captured in Canopy Traps

Moths collected in canopy traps placed several meters above the forest canopy are believed to be representative of emigrating SBW adults [24]. The sex, forewing length and area, and weight of SBW moths caught in those traps at Lac des Huit Milles in 1989–1990 were recorded. The forewing surface area averaged 0.361 ± 0.047 cm^2 (n = 1044) in males and 0.421 ± 0.063 cm^2 (n = 1024) in females, a significant difference (F = 599; df = 1; $p < 0.001$). The forewing surface area was normally distributed in males (AD = 1.039; $p = 0.01$) and near-normally distributed in females (AD = 0.587; $p = 0.126$). For the same moths, dry weight averaged 0.00475 ± 0.00143 g in males and 0.00684 ± 0.00287 g in females. We found a curvilinear relationship between wing surface area and dry weight, with a significant effect of sex on intercept (F = 7.15; df = 1, 2061; $p = 0.008$), but no effect of sex on slope (F = 1.56; df = 1, 206; $p = 0.212$):

$$M = \begin{cases} e^{-6.697+3.626A}\ \varepsilon \text{ for males} \\ e^{-6.582+3.626A}\ \varepsilon \text{ for females} \end{cases} \quad (4)$$

where the distribution of error ε is approximately lognormal with mean of 1 and standard deviation $\sigma_\varepsilon = 0.206$ for males (AD = 7.3; $p < 0.005$) and $\sigma_\varepsilon = 0.289$ for females (AD = 6.4; $p < 0.005$) ($R^2 = 0.95$ for both; Figure 3).

Both the forewing surface area and dry weight of moths caught in canopy traps decreased during the flight season for both sexes (Figure 4a). It has been suggested that this gradual drop in wing surface area during the flight season results from slower development and generally later emergence of smaller individuals as a possible result of parasitism, poor food quality, and/or low food quantity in the larval stages [24]. Among males, dry weight decreased at nearly the same rate as wing area, but among females, the dry weight loss was steeper than the decrease of wing area, which we attribute to the females losing substantial body weight with oviposition over the course of the flight season.

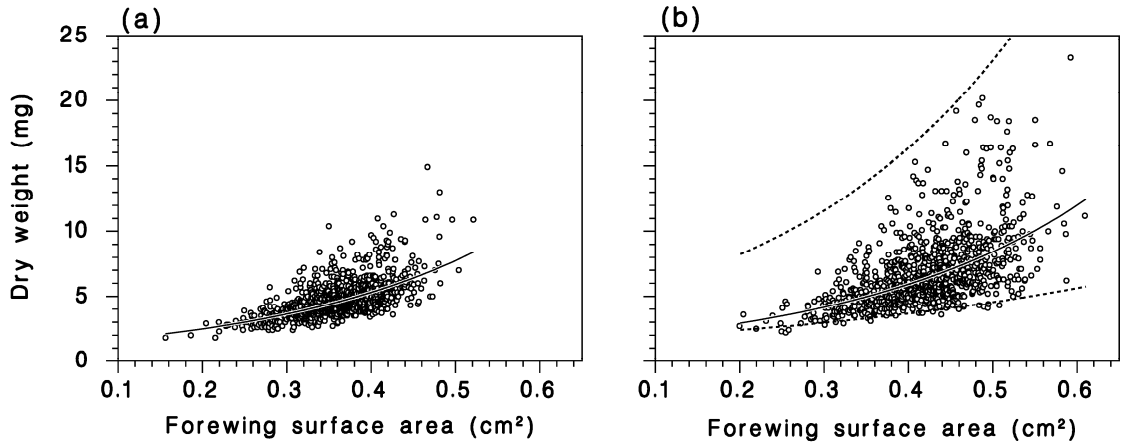

Figure 3. Relationship between dry weight (g) and forewing surface area (cm^2) in (**a**) male and (**b**) female spruce budworm (SBW) moths caught in canopy traps over the entire flight season at Lac des Huit-Milles, 1989–1990. Solid lines represent the fitted relationships for (**a**) males and (**b**) females, as in Equation (4). Dotted lines in (**b**) represent theoretical bounds for females based on gravidity using Equation (3).

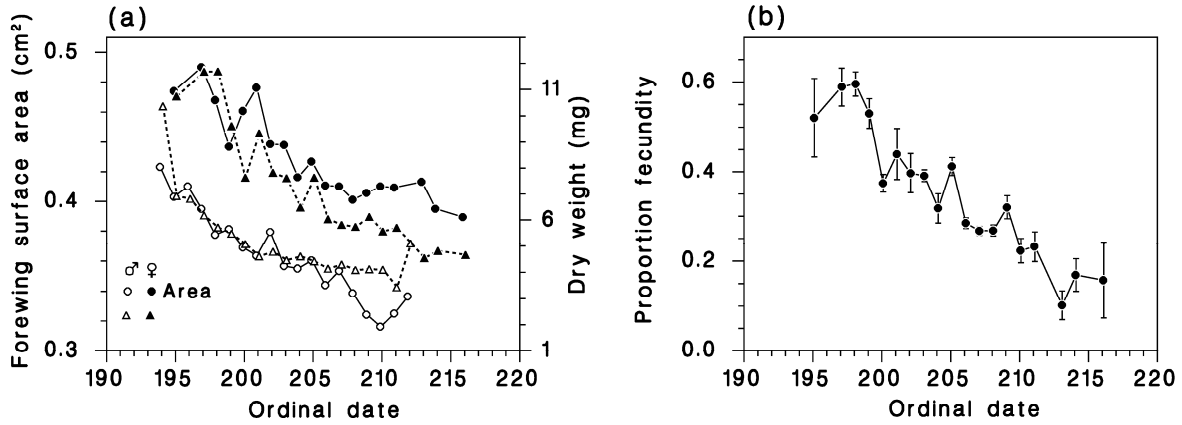

Figure 4. (**a**) Changes in average forewing surface area and dry weight over the flight season in males and females. (**b**) Gravidity of females calculated with Equation (5) (vertical bars represent the standard error of the mean). Moths caught in canopy traps at Lac des Huit-Milles, 1989–1990.

Rearranged, Equation (3) was used to estimate the diminishing gravidity G of females collected over time in the canopy traps at Lac des Huit-Milles during the moth flight season (Figure 4b):

$$G = \frac{\ln(M) + 6.4648 - 2.14A}{0.9736 + 1.3049A} \quad (5)$$

The observed distribution of gravidity among those females had an overall mean of $G = 0.33 \pm 0.19$ ($n = 1023$), very similar to the distribution reported in the work of [9] (their Table VI) with $G = 0.31 \pm 0.17$ ($n = 854$), assuming an average fecundity of 200 eggs/female.

2.2.3. Defoliation at the Individual Level

Individual SBW larvae cause and experience defoliation at the tree shoot (branchlet) level. To enable the generation of realistic individual-level defoliation exposures from stand-level defoliation estimates, we measured defoliation using Fettes' method [27] in the lower St. Lawrence stands during 2010–2015 from 45 cm branch samples taken at the end of the SBW egg hatch. Defoliation was assessed on the 20 most apical shoots of each branch. These data were used to relate average (stand-level)

defoliation to the frequency distribution of defoliation at the shoot level (and, by extension, the individual insect's level) using a Beta (α, β) distribution [28]. The parameters of this distribution are estimated by

$$\alpha = \mu_d\left(\frac{\mu_d(1-\mu_d)}{\sigma_d^2} - 1\right) \text{ and } \beta = (1-\mu_d)\left(\frac{\mu_d(1-\mu_d)}{\sigma_d^2} - 1\right) \quad (6)$$

where μ_d and σ_d are the mean and standard deviation of defoliation d (a proportion between 0 and 1) measured at the shoot level. We also obtained an empirical relationship between the mean and variance of defoliation values from these foliage samples using ordinary least-squares regression:

$$\sigma_d^2 = 0.008101 + 0.5289\mu_d - 0.5228\mu_d^2 \left(R^2 = 0.953\right), \quad (7)$$

where mean defoliation μ_d is expressed as a proportion rather than a percentage (Figure 5a). The observed and corresponding Beta distributions of shoot-level defoliation match very well (Figure 5b–g). The results indicate that there is large variability in the degree of food competition among larvae when defoliation is in the range d = 0.2–0.8. When defoliation is extreme (d > 0.9), the vast majority of individuals experience food limitation. In the individual-based model, these defoliation-dependent scaling distributions affect the distributions of moth weight and fecundity across a range of source populations and landscapes.

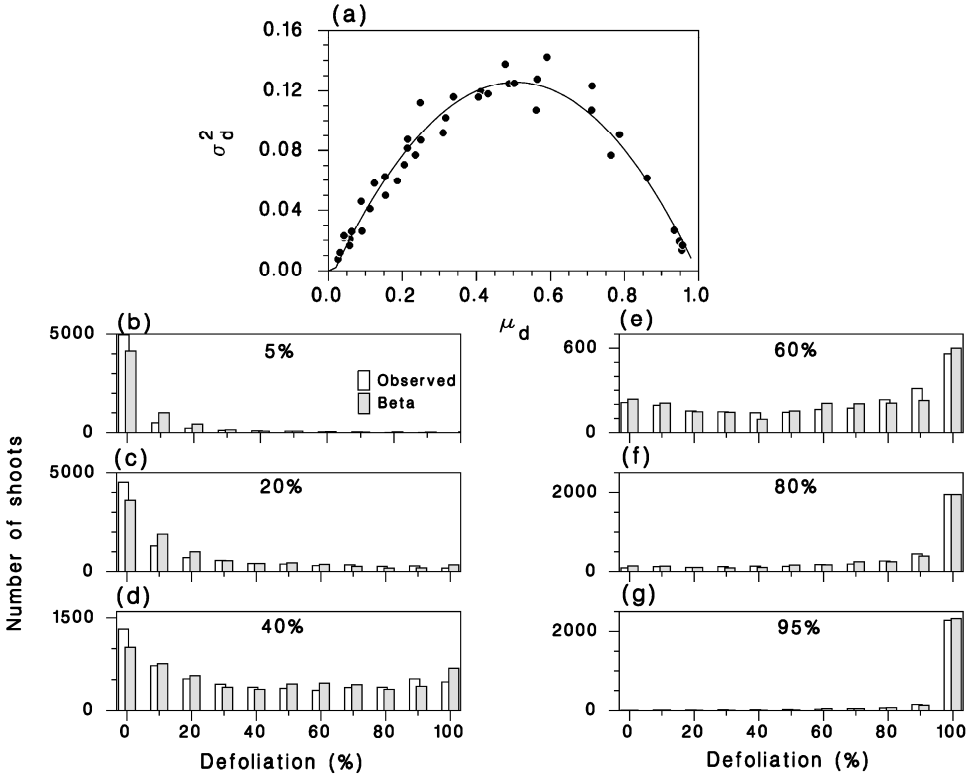

Figure 5. (**a**) Relationship between stand-level variance σ_d^2 and mean μ_d defoliation expressed as a proportion, with the line from Equation (7). (**b**–**g**) Observed and Beta frequencies of shoot-level defoliation for ranges of stand-level defoliation from 5% to 95%. Data from balsam fir in the lower St. Lawrence region, 2012–2015.

2.3. Flight Model

Using a table of in-flight wingbeat frequencies from 160 species of flying insects [29], Deakin [30] developed a simple double-allometric relationship to describe these observations with high accuracy:

$$\nu_L = K\frac{\sqrt{M}}{A} \tag{8}$$

where K is a proportionality constant (Hz cm^2 g$^{-1/2}$), M is mass (g), A is the surface area of a single forewing (cm^2), and ν_L (Hz) is the wingbeat frequency recorded at 20–24 °C. We assume here that ν_L is the minimum wingbeat required for the insect to lift off.

The wingbeat frequency of moths observed by the authors of [9] in sustained flight over radar was in the range ν_S = 25–42 Hz. We used an iterative numerical optimization procedure to maximize the overlap between this range and the wingbeat frequencies calculated with Equation (8). This procedure involved calculating the liftoff wingbeat frequency ν_L of all moths in the samples collected from canopy traps in Lac des Huit-Milles in 1989–1990, varying the value of K between 165 and 175 (in steps of 0.1), and selecting the value that provided the maximum overlap with the range ν_S = 25–42 Hz. With this procedure, we obtained K = 167.5 ± 0.05 Hz cm^2 g$^{-1/2}$, yielding 94.4% of overlap. The distribution of liftoff wingbeat frequencies for male and female moths in our sample from canopy traps is very similar (Figure 6a). Using this estimate of K, the liftoff wingbeat frequencies of females from our sample of pupae illustrate that liftoff is far easier for spent females than for gravid females (Figure 6b); while spent females require typical liftoff wingbeat frequencies ν_L < 30 Hz, fully gravid females can have liftoff wingbeat frequencies ν_L > 50 Hz, beyond the range observed by the authors of [9] and supporting the observation that gravid females must typically deposit their first eggs in the natal site before attempting migratory flight.

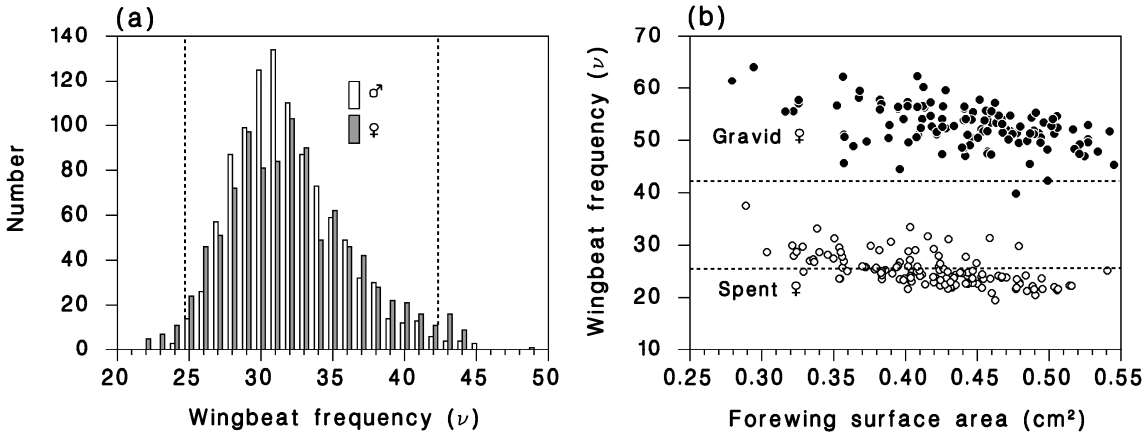

Figure 6. Liftoff wingbeat frequencies calculated from dry weight and forewing surface area with Equation (8) using K = 167.5 Hz. (**a**) Distribution of wingbeat frequencies of male and female moths caught in canopy traps. Vertical dotted lines: observed range of wingbeat frequencies of migrating budworm moths (ν = 25–42 Hz according to the authors of [9]). (**b**) Liftoff wingbeat frequencies of fully gravid (●) and spent (○) females from observations at Lac des Huit-Milles, 1989–1990.

As with many insect physiological processes, the rate at which an insect can beat its wings is a function of ambient temperature [31–37]. There is some evidence that wingbeat frequency may actually decrease at high temperatures in some moths [37], but this has not been seen in other insects. Because thermal responses in insects are non-linear [38], we use a sigmoid-shaped logistic curve where wingbeat increases exponentially at low temperatures, then asymptotically approaches a maximum (ν_{max}) at higher temperatures:

$$\nu(T) = \frac{\nu_{max}}{1 + \exp^{-b(T-a)}} \tag{9}$$

where T is ambient temperature (°C), ν_{max} is a species-specific maximum wingbeat frequency (Hz), a is the midpoint temperature of the response (°C), and b is the spread of that response with respect to temperature ($°C^{-1}$). In small moths, it seems that wing fanning does not generate enough heat to raise the insect's body temperature significantly above that of the air around it, so thermoregulation can be ignored [32]. In our model, we ignore SBW thermoregulation.

Here, we assume that the wingbeat of an airborne individual determines whether it ascends (when $\nu(T) \geq \nu_L$) or descends (when $\nu(T) < \nu_L$) in the atmospheric boundary layer with a given temperature profile. In this model, moths cannot lift off at a temperature $T < T_L$ because they cannot beat their wings fast enough. This leads to limitations on the time of SBW liftoff as the near-surface temperature decreases from sunset through the evening [17].

After liftoff, an airborne moth climbs through the air column until it reaches the altitude at which its wingbeat frequency matches ν_L, which occurs at the temperature T_L:

$$T_L = a - b \ln\left(\frac{A\,\nu_{max}}{K\sqrt{M}} - 1\right) \tag{10}$$

Once the moth has reached that altitude, we introduce an energy conservation factor Δ_ν that allows the insect to settle into sustained flight at an altitude where the temperature T_S is somewhat higher than T_L, but without increasing its wingbeat frequency as in Equation (9). We define $0 < \Delta_\nu \leq 1$ as a proportional reduction from physiological maximum wingbeat frequency ν_{max}, such that

$$\nu_L = \nu(T_S)\,\Delta_\nu \tag{11}$$

Thus, the altitude at which sustained flight occurs is that where

$$T_S = a - b \ln\left(\frac{\Delta_\nu}{K}\frac{A\,\nu_{max}}{\sqrt{M}} - 1\right) \tag{12}$$

If the air temperature changes while the insect is in flight, the individual must settle at a new altitude that satisfies Equation (12). For a typical temperature profile above the nocturnal inversion, this higher temperature occurs at a slightly lower flight altitude. However, as the ambient temperature drops below the moth's required T_S at all reachable altitudes, the airborne insect will continue to descend in search of T_S until it lands. Equation (12) tells us that the temperature at which an insect can fly depends on its weight and wing surface area, and that, other than K in Equation (8), there are four parameters that need to be estimated to complete this description: ν_{max}, a, and b in Equations (9) and (10) and Δ_ν in Equations (11) and (12).

We are aware of three sets of data with flight activity observations recorded over a wide range of temperature for the SBW. Flights by mated, egg-laying females have been observed in the laboratory [39], where the lower temperature threshold for flight was 15 °C. However, these were not observations of migratory flight. The late C.J. Sanders observed from tall scaffolds the number of males "buzzing" around the upper crowns of selected balsam fir trees in a mixed stand near Black Sturgeon Lake, Ontario, in 1987 (unpublished data). Observations of buzzing males and the ambient temperature were noted during five-minute periods, replicated several times per hour, during the peak evening period of moth activity on successive nights. From those observations, we calculated the average number of moths buzzing for temperature classes of 2 °C width in the range 12–30 °C, with very few males observed buzzing below 14 °C. However, these observations do not provide information on the value of ν_{max}, and it is not yet entirely clear how the wingbeat frequency of male buzzing at upper tree crowns is related to migration flight.

The third dataset provides more useful information. Through a complex procedure of foliage sampling and radar observations, the proportion of available egg-laying females that emigrated on several evenings during peak flight activity in 1973–1974 was estimated for two locations in central New Brunswick [40]. The authors defined as "available" those females that were at least two days

old and had begun oviposition. They also recorded the top-of-canopy temperature at 20:40 (sunset) every evening (n = 24). While these observations do not provide wingbeat frequencies, the observers were specifically concerned with females attempting migratory flight. Using our morphometric measurements (M and A) from females caught in canopy traps at Lac des Huit-Milles in 1989–1990 that were also (presumably) attempting emigration, we calculated the proportion of females that could lift off as a function of temperature and compared those calculations with the work of [40].

Finally, we used a grid-search optimization method to estimate values for the three unknown parameters of Equation (9): ν_{max}, a, and b at resolutions of 0.5, 0.1, and 0.005, respectively. We selected the values that minimized the residual sum of squares between the observed proportions [40] and those calculated from the liftoff wingbeat frequencies provided by Equation (8) for females caught in canopy traps at Lac des Huit-Milles in 1989–1990. We used the value of K obtained from Equation (8) above in our parameter estimation for Equation (9). Our best parameter estimates were ν_{max} = 72.5 ± 0.5 Hz, a = 23.0 ± 0.1 °C, and b = 0.115 ± 0.005 °C^{-1}, yielding the lowest residual sum of squares (R^2 = 0.561; line in Figure 7a). There was a high correlation between calculated wingbeat frequency and the observations of male SBWs buzzing around the crowns of host trees near Black Sturgeon Lake in 1987 (r = 0.89; Figure 7b).

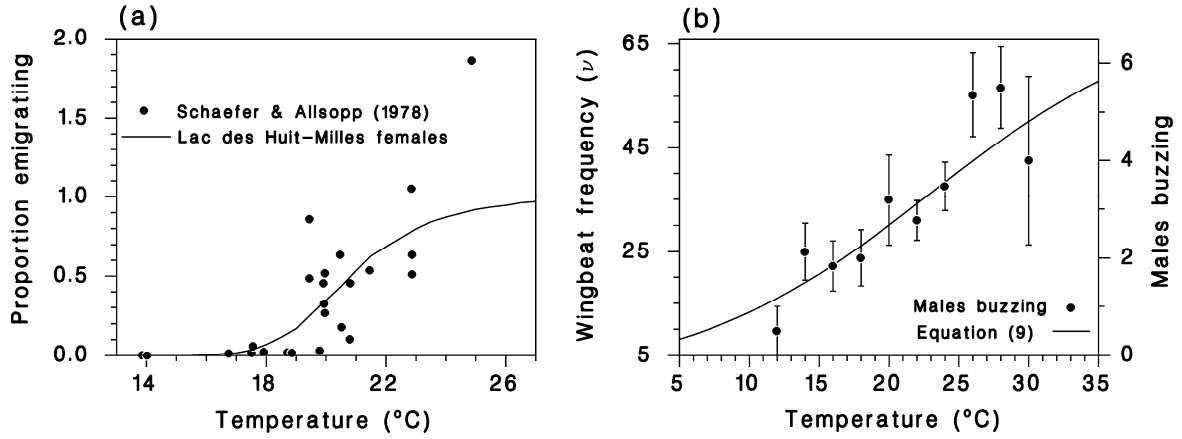

Figure 7. (**a**) Influence of temperature on proportion of females emigrating (circles: observations [39], line: prediction for females caught at Lac des Huit-Milles, 1989–1990); (**b**) observed temperatures and numbers of "buzzing" males (circles, from unpublished data of C.J. Sanders) and corresponding wingbeat frequency calculated with Equation (9) (solid line).

2.4. Flight Model Simulations

We used the above relations to simulate flight for 10,000 individual SBW moths (50% female) in idealized atmospheric boundary layer conditions. Each individual was assigned a random value of forewing surface area according to sex from normal distributions based on the observations for male and female moths collected in canopy traps at Lac des Huit-Milles in 1989–1990 (males 0.361 ± 0.047 cm^2; females 0.421 ± 0.063 cm^2). From those assigned forewing surface areas, we calculated the dry weight for each individual with Equation (4) using a lognormally-distributed ε error term with mean of 1 and standard deviations of 0.206 for males and 0.289 for females. We calculated female fecundity using Equations (1) and (2), and gravidity using Equation (5). We then calculated the liftoff wingbeat frequency ν_L for each moth using Equation (8), the liftoff temperature T_L with Equation (10), and the sustained flight temperature T_S with Equation (12) for two values of Δ_ν (1.0 and 0.85). When Δ_ν = 1, the liftoff temperature T_L and sustained flight temperature T_S are identical. As Δ_ν decreases, $T_S > T_L$ and sustained flight requires increasingly warmer temperatures relative to liftoff conditions.

To simulate the progression of flight under realistic temperature conditions, we generated an hourly time series of idealized air temperature profiles for the lower 1500 m of the atmospheric boundary layer from 20:00 (sunset) through 05:00 the next morning (Figure 8). This profile time

series imitates the evolution of a nocturnal temperature inversion (i.e., where temperature increases with altitude) owing to surface radiative cooling that is typical of a calm, clear summer night in temperate North America. This inversion appears near the surface at sunset, then increases in depth and dissipates gradually overnight (Figure 8; cf. observed profiles in the work of [41]).

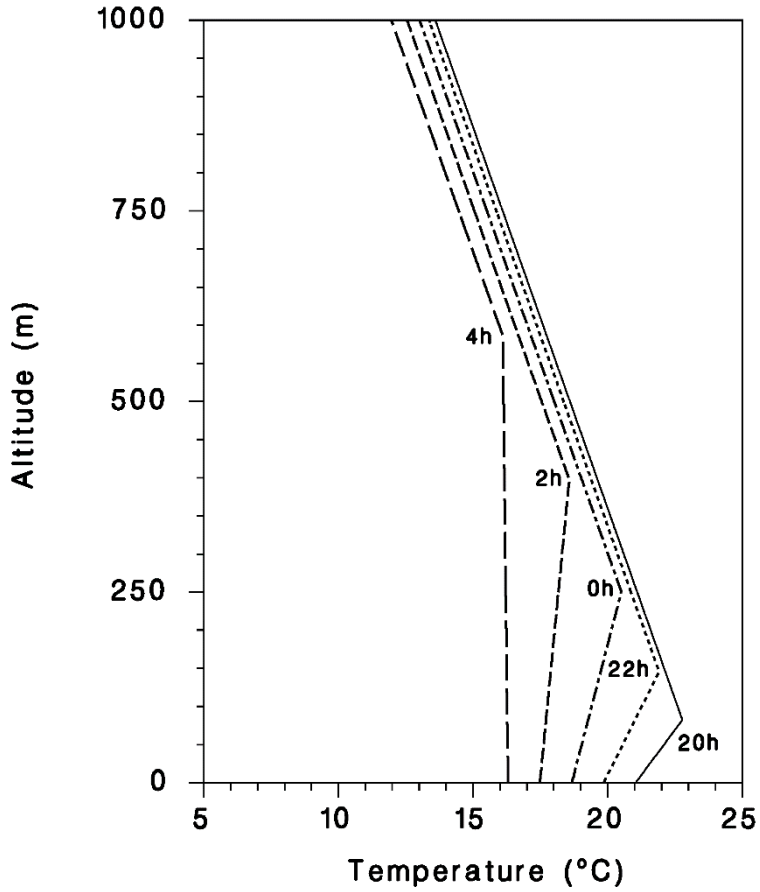

Figure 8. Idealized (archetypal) evening transition and nocturnal boundary layer temperature profile for a clear, calm summer night in northern temperate latitudes. The inversion develops from surface radiative cooling that begins near sunset, increases in depth, and dissipates gradually by early morning.

The evening boundary layer transition and evolution of the nocturnal inversion, as well as their potential roles in SBW migratory flight around sunset, are discussed further in a companion paper [17]. Here, we have specified no wind profile for our flight simulations, choosing instead to focus solely on temperature-related influences on SBW flight. We specify that all moths attempt to lift off at sunset. Those moths that can lift off, where $T > T_L$ at the surface, either reach the altitude where temperature allows their sustained flight or, not finding such a level, return to the ground immediately. At each hour of the simulation, we recorded the vertical distributions of moth density, sex ratio, and gravidity (proportion of initial fecundity) carried by flying females. In the simulations presented here, we allow the moths to reach their cruising altitude immediately upon liftoff, as the time step is 1 h, long enough for them to reach it. When a temperature inversion exists, the simulated moths settle into sustained flight above the inversion. In a more realistic simulation context, with actual temperature data, we use a 5–10 min time step. In that case, the ascent rate is proportional to the difference between the wingbeat frequency for the air temperature at the current location $\nu(T)$ and the sustained flight wingbeat frequency ν_S as $Vz = \alpha[\nu(T) - \nu_S]$ where $\alpha = 0.11$ m s^{-1} Hz^{-1}, yielding a range of about 0–2 m/s, commensurate with observed ascent rates [9].

3. Simulation Results

The vertical distribution of flying moths varied over time and with the value of Δ_ν (Figure 9a,d). Overall, females tended toward sustained flight at higher altitudes than males (Figure 9b,e), although the heavier females (i.e., those with greater gravidity) generally remained at lower flight altitudes (Figure 9c,f) because of their greater weight relative to partially or totally spent females. In the $\Delta_\nu = 1$ simulation, nearly 60% of moths achieved sustained flight, compared with only 40% when $\Delta_\nu = 0.85$. The number of flying moths decreased gradually overnight as the air column cooled, and the mode (peak concentration) of flying SBW ascended with time. With $\Delta_\nu = 1$, the mode of the vertical distribution of moths in flight remained ~200 m above the top of the surface inversion layer, while it descended to the top of the inversion with $\Delta_\nu = 0.85$. With $\Delta_\nu = 0.85$, the flight cloud lost males more quickly and became proportionally more populated by low-gravidity females over the evening.

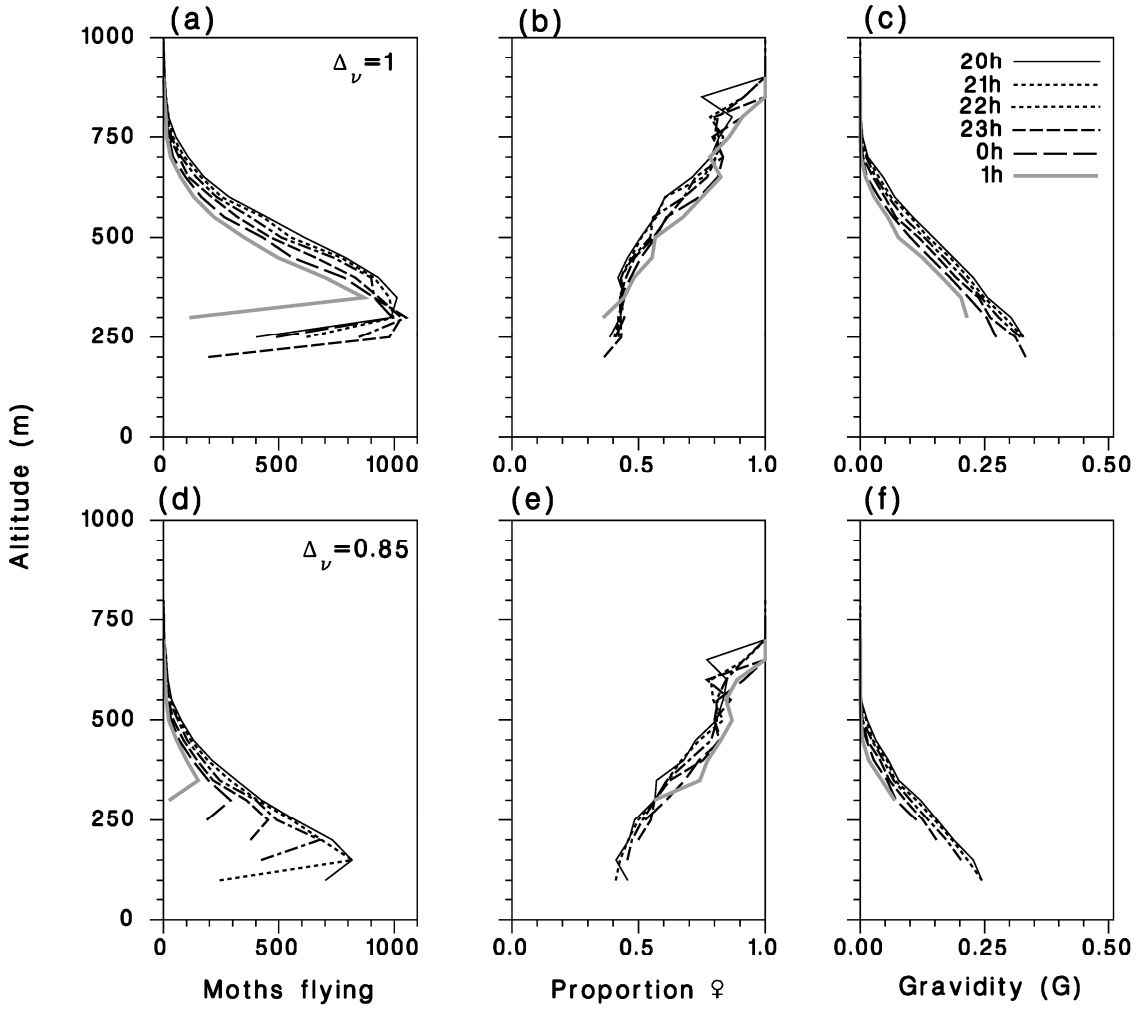

Figure 9. Hourly vertical density profiles of simulated migrating moths between liftoff at 20:00 (sunset) and 01:00 the next morning. Top row: $\Delta_\nu = 1.0$; bottom row: $\Delta_\nu = 0.85$. (**a**,**d**) Number of moths flying. (**b**,**e**) Proportion female. (**c**,**f**) Gravidity, the proportion of initial fecundity carried by females.

These simulation results are summarized over the entire simulation period in Figure 10. Most moths flew early in the evening while temperatures were highest, and their numbers diminished over the night as the temperature decreased throughout the specified boundary layer profile (Figure 10a). A smaller value of Δ_ν led to a decrease in the number of moths that remained airborne and the overall duration of the flight period (Figure 10a). The average altitude of airborne moths changed over time; heavier individuals, especially the most gravid females, were forced to land earlier as temperature

decreased, leaving the males and less-gravid females in the flight concentration profile (Figure 10b). In addition, a smaller value of Δ_ν led to a lower mean flight altitude through much of the night, as the airborne moths sought warmer air for sustained flight, until only the least-gravid females remained airborne near the top of the profile at the end of the night (Figure 10b). Overall, there are more airborne females than males, which corresponds to observations of a female-biased sex ratio among migrant moths [9]. However, the proportion of females among airborne moths in both simulations increased during the flight period, as males generally landed earlier than the less-gravid females (Figure 10c). This biased sex ratio is the result of different weight to wing surface area relationships in males and females. As the night progressed, the overall gravidity of migrating females decreased as heavier females were forced to land earlier. With a smaller value of Δ_ν, egg loads carried by migrating females were even lower as the more-gravid females found sustained flight more difficult and landed earlier than their less-gravid counterparts (Figure 10d).

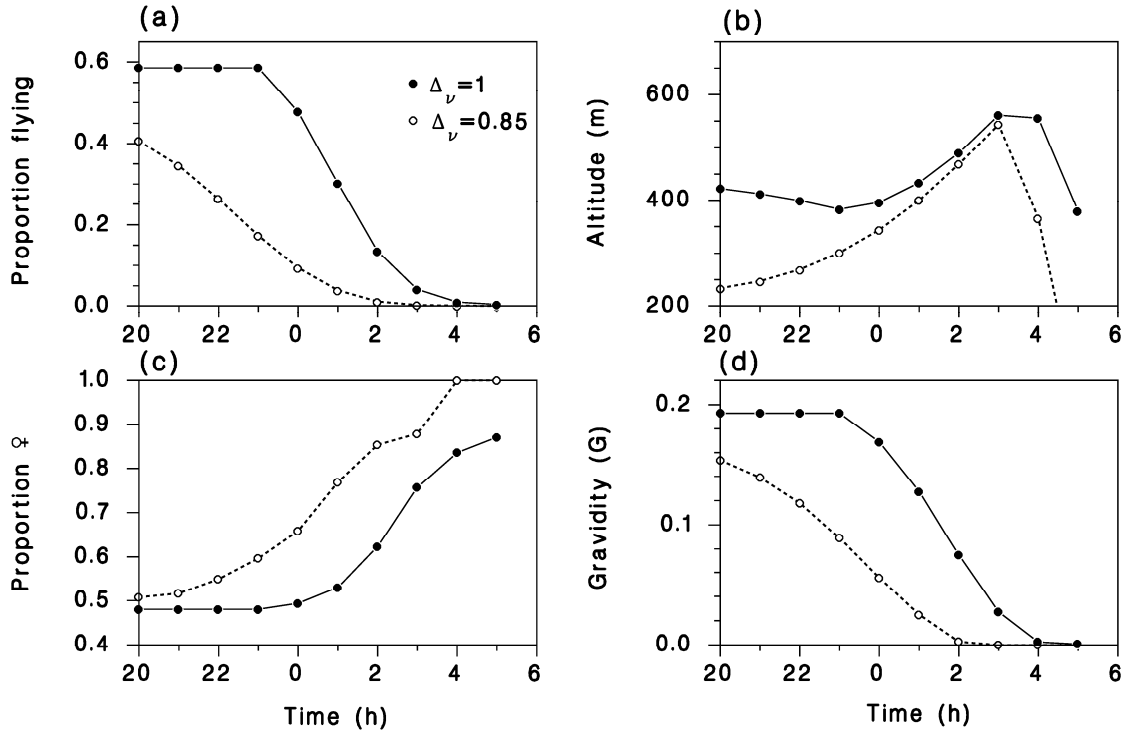

Figure 10. Summary of simulated migratory flights. (**a**) Proportion of moths in flight. (**b**) Mean flight altitude. (**c**) Proportion female among migrating moths. (**d**) Gravidity, the proportion of initial fecundity carried by migrating females. ●: $\Delta_\nu = 1.0$; ○: $\Delta_\nu = 0.85$.

4. Discussion

Our explicit use of empirically-derived biophysical relationships between SBW moth size and weight, gravidity, wingbeat frequency, and temperature in this model improves greatly upon previous individual-based models of SBW migratory flight [21]. Fundamental determinants of liftoff, cruising altitude, and descent are emergent properties of interactions between modeled moth flight behaviors and the evolving surface conditions and boundary layer temperature profile. The empirical analyses underlying our flight model are highly consistent with known SBW life history [9], and the consequent model provides additional insight into other aspects of its aerobiology that have remained poorly understood.

Our results suggest that fully gravid females have liftoff wingbeat frequencies $\nu_L > 50$ Hz (outside the reported range of ν = 25–42 Hz in [9]), while spent females have much lower liftoff wingbeat frequencies ($\nu_L < 30$ Hz). This difference, which can be attributed to the weight of eggs carried by the female, explains why fully gravid females do not readily emigrate [13,14,39,42,43]. However, females

from severely defoliated stands are smaller, lighter, and have lower fecundity than well-fed females. Those lighter females can fly soon after emergence without laying any eggs [15,16], an observation also consistent with our model formulation. Simulated vertical density profiles (Figure 9a) are further consistent with recent radar observations of SBW mass migration events [19]. Indeed, temperature responses by migrating insects remain among one of the most plausible factors of the atmosphere influencing the formation of flight layers in and above the atmospheric boundary layer across a broad range of insect taxa and flight seasons [6,18,44]. Temperature constraints on flight may further explain temperature dependence in the timing of liftoff relative to sunset and dusk [9], as we have explored in a companion paper [17].

These simulation results, despite their idealized setting, suggest several features of SBW dispersal that may be consequential to our understanding of SBW outbreak spatiotemporal dynamics. The fundamental premise of our individual-based model is that moth flight altitude is determined primarily by interaction between the air temperature profile in the atmospheric boundary layer and the individual moth's ability to maintain a sufficient wingbeat frequency to remain airborne. Depending on the temperature profile and its trend through the night, we found that most moths eventually land because of cool air at some time well before sunrise, as observed with radar [9]. We can thus conclude from our simulations that flight duration results from an interaction between air temperature and the moth's weight and size. Though we have not specified a boundary layer wind profile along with the simulation temperature profile, we can still draw some conclusions from the flight duration itself. For example, the most-gravid females carrying significant egg loads fly for comparatively short periods and hence short distances. Perhaps counterintuitively, some females fly higher (and longer) than males, but those females are less gravid with smaller egg loads (Figure 10c,d). These outcomes suggest some limitations on the ability of the adult SBW to disperse eggs over the full range of distances that can be reached by the source population in a given location. However, distance limitations can also change over the flight season, with late-emerging adults generally being lighter and thus able to attain a greater flight range under generally warmer (and thus even more favorable) temperature conditions. Source populations in severely defoliated regions will likewise emerge to be smaller and lighter, with more-gravid females having an increased ability to lift off and fly longer distances in those warmer conditions.

Absent from our simulations, and from the discussion thus far, are the potential effects of a variable wind profile in the atmospheric boundary layer on flight distances. Where temperature is a principal determinant of flight altitude, a demographic sorting occurs in the vertical profile of moth concentration. The most-gravid females generally remain at the top of the surface boundary layer inversion (Figure 9c,f) during their flight, while males and less-gravid females generally settle into sustained flight above that level, with males present throughout the profile. Boundary layer wind profiles in the same seasons that produce our idealized temperature profile have a generally similar shape. Winds are typically slower near the surface (due to surface friction, and not accounting here for possible directional changes), and increase with altitude to a possible maximum just above the top of the boundary layer inversion. There, a low-level jet can form in otherwise calm synoptic conditions on some nights [45,46] and with often diminishing wind speeds above that maximum.

The vertical demographic sorting effect of the ambient temperature profile is thus compounded by the boundary layer wind profile, resulting in further sorting over the distance travelled from the source region. More-gravid females fly at the top of the surface inversion layer, in or near the greatest wind speeds, and may have a greater flight range despite landing first because of overall boundary layer cooling. The largest concentration of males generally fly lowest, potentially below the wind maximum, and land within the shortest distance, but with considerable spread over the entire flight range as higher-flying males reach greater distances; less-gravid females, flying at and just above the greatest wind speeds, can reach the greatest distances from the source area before landing. In terms of egg deposition by migrants, a distinct pattern emerges from these (admittedly idealized) considerations. The highest concentration of eggs (as much as half of original fecundity) is deposited in the natal area

by the gravid females who are too heavy to fly upon emergence. Adjacent to that natal area, there is a low concentration of egg deposition where migration landings are dominated by short-flying males, out to a distance where the most-gravid females land and form a secondary concentration peak in egg deposition, which diminishes slowly with distance as less-gravid females land and deposit their eggs at lower concentrations. The coherence of this pattern in any particular direction from the source region remains contingent on wind direction, its persistence through the evening and night, and its variability with height in the atmospheric boundary layer. The overall effects of these combined emergent properties on the spatiotemporal dynamics of SBW outbreaks are yet to be determined, but our individual-based model holds promise for the examination of the structure and consequences of dispersal events under both current and potential future conditions [47].

An example of the importance of demographic details (i.e., males and females, and relative gravidity of females) occurs in consideration of convergent atmospheric wind patterns [9]. Dispersal in general tends to dilute the concentrations of SBW from the initial source areas as moth landings occur across a much broader region. However, various features of weather, topography, and land–water interfaces often create wind convergence zones that can concentrate flying insects [48]. Examples of mesoscale concentration of migrating SBW moths associated with sea breezes have been observed via radar in a number of instances (e.g., the works of [49,50]), and smaller-scale convergence zones associated with topography have been shown to concentrate other species of flying insects (e.g., the work of [51]). If such concentrations are also associated with changes in boundary layer temperature, as often occurs in valley regions at night, the density of landing insects can be far greater in those locations and the enhanced concentration of deposited eggs can lead to greater defoliation and potential for outbreak initialization in subsequent years [51]. Given a general assumption of dispersal spread with migration distance, mesoscale convergence needs to occur close to primary source areas for such concentrations to occur. Localized convergence associated with topography occurs most strongly close to the ground [48], generally where greater numbers of more-gravid females can fly, and, as we have demonstrated, flight distance from the source can effectively select for critical demographic factors such as male/female ratios and female gravidity.

5. Conclusions

This model of SBW migratory flight, combined with a model predicting the circadian rhythm of liftoff times [17], constitutes significant progress in our understanding of the interactions between SBW and its environment and the emergent effects of those interactions on SBW dispersal and migration. Investigations of model behavior in real weather conditions, over actual terrain, and in comparisons with various sources of observations such as Doppler radar [19] and trap networks are needed to advance the development, calibration, and validation of our model framework and its assumptions. Of the several model parameters estimated here, Δ_v remains the most uncertain; traditional observations are not sufficient for its estimation, leading us to specify its value in the flight simulations described above. Its value could be defined better by comparing sets of observed and simulated vertical distributions of migrating moths. The parameters of Equation (9) were obtained somewhat indirectly, from field observations of emigrating moths [40]. A better understanding of the shape of the relationship between temperature and wingbeat frequency in Equation (9) for both male and female SBW could provide further significant improvement of our individual-based model. One simplifying assumption, in need of verification, is the absence of thermoregulation in SBW moths. It is possible that moths may warm their thoracic muscles so they can lift off and migrate in cold temperatures, and it is still possible (contrary to the work of [32]) that sustained flight further warms those muscles, changing the (still uncertain) efficiency and energy consumption of SBW physiological activity over the course of the flight. Finally, the morphometric data presented here (Figure 1) come from a single location (Lac des Huit Milles in Quebec, Canada) in 1989 and 1990, but we know of additional datasets relating wing size and weight in gravid and spent females from which we may

obtain a better understanding of the interannual variation in that relationship that is not fully explained by defoliation. Incorporating these additional data would undoubtedly improve our model.

Despite these remaining uncertainties, we now have a well-founded process model to describe three of the principal aerobiological stages of moth migration for the SBW: launch/ascent, horizontal transport, and descent/landing [21,52]. Such a model can now be linked to a model of SBW phenology [46], functions defining circadian rhythm of migration flight behavior [17], maps of known populations and/or defoliation activity, and weather model outputs [53] to simulate the entire migration process in near-real-time. Comparison of the outputs of such a model with observations from ground-based trap networks and radar data could be used to calibrate the least understood model parameters, point to avenues for model improvement, and validate model predictions. Such an integrated model might ultimately be used to predict mass migration events and the distribution of SBW eggs to assist in the management of potential SBW outbreaks.

Author Contributions: Conceptualization, J.R., J.D., and R.S.-A.; Methodology, J.R. and R.S.-A.; Software, R.S.-A.; Validation, J.R., R.S.-A., and B.R.S.; Formal Analysis, J.R.; Investigation, J.R. and J.D.; Resources, J.D. and J.R.; Data Curation, J.R.; Writing—Original Draft Preparation, J.R., J.D., B.R.S., and M.G.; Writing—Review & Editing, J.R., B.R.S., J.D., M.G., and R.S.-A.; Visualization, J.R.; Supervision, J.R. and J.D.; Project Administration, J.R. and J.D.; Funding Acquisition, J.R., J.D., and B.R.S.

Funding: This research was funded by the natural resources and forest departments of Newfoundland, Nova Scotia, New Brunswick, Quebec, Ontario, Manitoba, Saskatchewan, Alberta, and British Columbia. Funds were also provided by the Atlantic Canada Opportunities Agency, and under the U.S./Canada Forest Health & Innovation Summit Initiative sponsored by the USDA Forest Service, Canadian Forest Service of Natural Resources Canada, and the U.S. Endowment for Forestry and Communities, with cooperation by SERG-International.

Acknowledgments: We thank Ariane Béchard, Alain Labrecque, and Pierre Therrien for their contributions to the field work, and Marc Rhainds (Canadian Forest Service, Atlantic Forestry Centre, Fredericton, NB) for discussions related to spruce budworm moth morphology and morphometry. M.G. wishes to acknowledge the support of Philip A. Townsend at the University of Wisconsin–Madison.

Conflicts of Interest: The authors declare no conflict of interest.

References

1. Johnson, C.G. *Migration and Dispersal of Insects by Flight*; Methuen & Co. Ltd.: London, UK, 1969; p. 763. [CrossRef]
2. Schowalter, T. *Insect Ecology: An Ecosystem Approach*, 4th ed.; Academic Press: London, UK, 2016; p. 774.
3. Den Boer, P.J. Spreading of risk and stabilization of animal numbers. *Acta Biotheor.* **1968**, *18*, 165–194. [CrossRef] [PubMed]
4. Dingle, H.; Drake, V.A. What is migration? *Bioscience* **2007**, *57*, 113–121. [CrossRef]
5. Chapman, J.W.; Drake, V.A.; Reynolds, D.R. Recent insights from radar studies of insect flight. *Ann. Rev. Entomol.* **2011**, *56*, 337–356. [CrossRef] [PubMed]
6. Drake, V.A. The vertical distribution of macro-insects migrating in the nocturnal boundary layer: A radar study. *Bound.-Layer Meteorol.* **1984**, *28*, 353–374. [CrossRef]
7. Riley, J.R.; Reynolds, D.R. A long-range migration of grasshoppers observed in the Sahelian zone of Mali by two radars. *J. Anim. Ecol.* **1983**, *52*, 167–183. [CrossRef]
8. Westbrook, J.K.; Nagoshi, R.N.; Meagher, R.L.; Fleischer, S.J.; Jairam, S. Modeling seasonal migration of fall armyworm moths. *Int. J. Biometeorol.* **2016**, *60*, 255–267. [CrossRef] [PubMed]
9. Greenbank, D.O.; Schaefer, G.W.; Rainey, R.C. Spruce budworm (Lepidoptera: Tortricidae) moth flight and dispersal: New understanding from canopy observations, radar, and aircraft. *Mem. Entomol. Soc. Can.* **1980**, *112*, 1–49. [CrossRef]
10. Gray, D.R.; MacKinnon, W.E. Outbreak patterns of the spruce budworm and their impacts in Canada. *For. Chron.* **2006**, *82*, 550–561. [CrossRef]
11. Régnière, J.; Delisle, J.; Pureswaran, D.S.; Trudel, R. Mate-finding Allee effect in spruce budworm population dynamics. *Entomol. Exp. Appl.* **2013**, *146*, 112–122. [CrossRef]
12. Régnière, J.; Cooke, B.J.; Béchard, A.; Dupont, A.; Therrien, P. Dynamics and management of rising spruce budworm populations. *Forests* **2019**, *10*, 748. [CrossRef]

13. Wellington, W.G.; Henson, W.R. Notes on the effects of physical factors on the spruce budworm, *Choristoneura fumiferana* (Clem.). *Can. Entomol.* **1947**, *79*, 168–170. [CrossRef]
14. Rhainds, M.; Kettela, E.G. Oviposition threshold for flight in an inter-reproductive migrant moth. *J. Insect Behav.* **2013**, *26*, 850–859. [CrossRef]
15. Blais, J.R. Effects of the destruction of the current year's foliage of balsam fir on the fecundity and habits of flight of the spruce budworm. *Can. Entomol.* **1953**, *85*, 446–448. [CrossRef]
16. Van Hezewijk, B.; Wertman, D.; Stewart, D.; Beliveau, C.; Cusson, M. Environmental and genetic influences on the dispersal propensity of spruce budworm (*Choristoneura fumiferana*). *Agric. For. Entomol.* **2018**, *20*, 433–441. [CrossRef]
17. Régnière, J.; Garcia, M.; St-Amant, R. Modeling migratory flight in the spruce budworm: Circadian rhythm. *Forests* **2019**. in revision.
18. Reynolds, D.R.; Chapman, J.W.; Edwards, A.S.; Smith, A.D.; Wood, C.R.; Barlow, J.F.; Woiwod, I.P. Radar studies of the vertical distribution of insects migrating over southern Britain: The influence of temperature inversions on nocturnal layer concentrations. *Bull. Entomol. Res.* **2005**, *95*, 259–274. [CrossRef] [PubMed]
19. Boulanger, Y.; Fabry, F.; Kilambi, A.; Pureswaran, D.S.; Sturtevant, B.R.; Saint-Amant, R. The use of weather surveillance radar and high-resolution three dimensional weather data to monitor a spruce budworm mass exodus flight. *Agric. For. Meteorol.* **2017**, *234*, 127–135. [CrossRef]
20. Anderson, D.P.; Sturtevant, B.R. Pattern analysis of eastern spruce budworm *Choristoneura fumiferana* dispersal. *Ecography* **2011**, *34*, 488–497. [CrossRef]
21. Sturtevant, B.R.; Achtemeier, G.L.; Charney, J.J.; Anderson, D.P.; Cooke, B.J.; Townsend, P.A. Long-distance dispersal of spruce budworm (*Choristoneura fumiferana* Clemens) in Minnesota (USA) and Ontario (Canada) via the atmospheric pathway. *Agric. For. Meteorol.* **2013**, *168*, 186–200. [CrossRef]
22. Dudley, R. *The Biomechanics of Insect Flight*; Princeton University Press: Princeton, NJ, USA, 2000.
23. Harvey, G.T. Mean weight and rearing performance of successive egg clusters of eastern spruce budworm (Lepidoptera: Tortricidae). *Can. Entomol.* **1977**, *109*, 487–496. [CrossRef]
24. Eveleigh, E.S.; Lucarotti, C.J.; McCarthy, P.C.; Morin, B.; Royama, T.; Thomas, A.W. Occurrence and effects of *Nosema fumiferanae* infections on adult spruce budworm caught above and within the forest canopy. *Agric. For. Entomol.* **2007**, *9*, 247–258. [CrossRef]
25. Nealis, V.G.; Régnière, J. Fecundity and recruitment of eggs during outbreaks of the spruce budworm. *Can. Entomol.* **2004**, *136*, 591–604. [CrossRef]
26. Anderson, T.W.; Darling, D.A. Asymptotic theory of certain "goodness-of-fit" criteria based on stochastic processes. *Ann. Math. Stat.* **1952**, *23*, 193–212. [CrossRef]
27. Sanders, C.J. A summary of current techniques used for sampling spruce budworm populations and estimating defoliation in eastern Canada. *Can. For. Serv. Info. Rep.* **1980**, *O-X-306*.
28. Gupta, A.K.; Nadarajah, S. *Handbook of Beta Distribution and Its Applications*; CRC Press: Boca Raton, FL, USA, 2004.
29. Byrne, D.N.; Buchmann, S.L.; Spangler, H.G. Relationship between wing loading, wingbeat frequency and body mass in homopterous insects. *J. Exp. Biol.* **1988**, *135*, 9–23.
30. Deakin, M.A.B. Formulae for insect wingbeat frequency. *J. Insect Sci.* **2010**, *10*, 96. [CrossRef] [PubMed]
31. Farnsworth, E.G. Effects of ambient temperature, humidity, and age on wing-beat frequency of *Periplaneta* species. *J. Insect Physiol.* **1972**, *18*, 827–839. [CrossRef]
32. Farmery, M.J. The effect of air temperature on wingbeat frequency of naturally flying armyworm moth (*Spodoptera exempta*). *Entomol. Exp. Appl.* **1982**, *32*, 193–194. [CrossRef]
33. Unwin, D.M.; Corbet, S.A. Wingbeat frequency, temperature and body size in bees and flies. *Physiol. Entomol.* **1984**, *9*, 115–121. [CrossRef]
34. Oertli, J.J. Relationship of wing beat frequency and temperature during takeoff flight in temperate-zone beetles. *J. Exp. Biol.* **1989**, *145*, 321–338.
35. Foster, J.A.; Robertson, R.M. Temperature dependency of wing-beat frequency in intact and deafferented locusts. *J. Exp. Biol.* **1992**, *162*, 295–312.
36. Snelling, E.P.; Seymour, R.S.; Matthews, G.D.; White, C.R. Maximum metabolic rate, relative lift, wingbeat frequency and stroke amplitude during tethered flight in the adult locust *Locusta migratoria*. *J. Exp. Biol.* **2012**, *215*, 3317–3323. [CrossRef] [PubMed]

37. Huang, J.; Zhang, G.; Wang, Y. Effects of age, ambient temperature and reproductive status on wing beat frequency of the rice leafroller *Cnaphalocrocis medinalis* (Guenée) (Lepidoptera: Crambidae). *Appl. Entomol. Zool.* **2013**, *48*, 499–505. [CrossRef]
38. Chuine, I.; Régnière, J. Process-based models of phenology for plants and animals. *Annu. Rev. Ecol. Evol. Syst.* **2017**, *48*, 159–182. [CrossRef]
39. Sanders, C.J.; Wallace, D.R.; Lucuik, G.S. Flight activity of female spruce budworm (Lepidoptera: Tortricidae) at constant temperatures in the laboratory. *Can. Entomol.* **1978**, *110*, 627–632. [CrossRef]
40. Schaefer, G.W.; Allsopp, K. *Analysis and Interpretation of Ground-Based and Airborne Radar Data Collection for the Spruce Budworm Dispersal Studies 1973–1976 Inclusive*; Final Report No. 4. Part B. The Effects of Canopy Temperature and Meteorological Factors on the Number of Moths Entering the Air Space; Ecological Physics Research Group, Cranfield Institute of Technology: Bedfordshire, UK, 1978.
41. Malingowski, J.; Atkinson, D.; Fochesatto, J.; Cherry, J.; Stevens, E. An observational study of radiation temperature inversions in Fairbanks, Alaska. *Polar Sci.* **2014**, *8*, 24–39. [CrossRef]
42. Wellington, W.G. The light reactions of the spruce budworm, *Choristoneura fumiferana* Clemens (Lepidoptera: Tortricidae). *Can. Entomol.* **1948**, *80*, 56–82. [CrossRef]
43. Henson, W.R. Mass flights of the spruce budworm. *Can. Entomol.* **1951**, *83*, 240. [CrossRef]
44. Wood, C.R.; Clark, S.J.; Barlow, J.F.; Chapman, J.W. Layers of nocturnal insect migrants at high-altitude: The influence of atmospheric conditions on their formation. *Agric. For. Entomol.* **2010**, *12*, 113–121. [CrossRef]
45. Angevine, W.M. Transitional, entraining, cloudy, and coastal boundary layers. *Acta Geophys.* **2008**, *56*, 2–20. [CrossRef]
46. Angevine, W.M.; Tjernström, M.; Žagar, M. Modeling of the coastal boundary layer and pollutant transport in New England. *J. Appl. Meteorol. Climatol.* **2006**, *45*, 137–154. [CrossRef]
47. Régnière, J.; St-Amant, R.; Duval, P. Predicting insect distributions under climate change from physiological responses: Spruce budworm as an example. *Biol. Invasions* **2012**, *14*, 1571–1586. [CrossRef]
48. Pedgley, A.D.E. Concentration of flying insects by the wind. *Philos. Trans. R. Soc. Lond. B* **1990**, *328*, 631–653. [CrossRef]
49. Schaefer, G.W. An airborne radar technique for the investigation and control of migrating pest species. *Philos. Trans. R. Soc. Lond. B* **1979**, *287*, 459–465. [CrossRef]
50. Dickinson, R.B.B.; Haggis, M.J.; Rainey, R.C. Spruce budworm moth flight and storms: Case study of a cold front system. *J. Clim. Appl. Meteorol.* **1983**, *22*, 278–286. [CrossRef]
51. Pedgley, D.E.; Reynolds, D.R.; Riley, J.R.; Tucker, M.R. Flying insects reveal small-scale wind systems. *Weather* **1982**, *37*, 295–306. [CrossRef]
52. Isard, S.A.; Gage, S.H.; Comtois, P.; Russo, J.M. Principles of the atmospheric pathway for invasive species applied to soybean rust. *BioScience* **2005**, *55*, 851–861. [CrossRef]
53. Benjamin, S.G.; Weygandt, S.S.; Brown, J.M.; Hu, M.; Alexander, C.R.; Smirnova, T.G.; Olson, J.B.; James, E.P.; Dowell, D.C.; Grell, G.A.; et al. A North American hourly assimilation and model forecast cycle: The Rapid Refresh. *Mon. Weather Rev.* **2016**, *144*, 1669–1694. [CrossRef]